Use of Bacterial Carpets to Enhance Mixing in Microfluidic Systems

Min Jun Kim[1]

Kenneth S. Breuer[2]
e-mail: kbreuer@brown.edu

Division of Engineering,
Brown University,
Providence, RI 02912

We demonstrate that flagellated bacteria can be utilized in surface arrays (carpets) to achieve mixing in a low-Reynolds number fluidic environment. The mixing performance of the system is quantified by measuring the diffusion of small tracer particles. We show that the mixing performance responds to modifications to the chemical and thermal environment of the system, which affects the metabolic activity of the bacteria. Although the mixing performance can be increased by the addition of glucose (food) to the surrounding buffer or by raising the buffer temperature, the initial augmentation is also accompanied by a faster decay in mixing performance, due to falling pH and oxygen starvation, both induced by the higher metabolic activity of the bacterial system.
[DOI: 10.1115/1.2427083]

Keywords: Serratia marcescens, microfluidics, mixing, diffusion bacterial carpet, glucose, temperature

1 Introduction

In a microfluidic environment, the small-scale and consequently low-Reynolds number flow regime leads to diffusion-limited, viscous-dominated dynamics. This has led to several engineering challenges, for example, how to pump fluids through a small system with optimum efficiency and how to enhance mixing between parallel streams of fluids. Mixing for chemical systems continues to be a challenge, although several concepts for laminar mixers have been proposed. Some of these techniques are associated with chaotic advection [1–3] in which the objective is to generate a chaotic cycle to stretch the two-fluid interface. Spatial methods [4–6] generate chaotic mixing using complex meandering channels, or ribbed channels. There have also been attempts at making temporal chaotic mixers at micro scale; however, these have tended to fail due to difficulties in finding a compact fluidic actuator that can be conveniently incorporated into a microfluidic system.

A novel approach for generating fluids mixing in small-scale devices is to employ the rotating flagella from bacteria as fluidic actuators [7]. Flagellated bacteria, such as *Escherichia coli* or *Serratia marcescens*, possess a remarkable motility system based on a reversible rotary motor [8,9]. Such bacteria typically have several flagella, each controlled by a separate, independent motor. When all the flagella rotate in a counterclockwise direction (its preferable sense of rotation), the flagella combine to form a bundle that propels the bacterium through the ambient fluid. A unique feature of bacterial flagellar motors is that they alternate between clockwise and counterclockwise rotation in a random manner, and this behavior leads to the execution of a random walk by bacteria as they move in the surrounding fluid. Thus, their natural behavior mimics, at the cellular level, the random motion of the classical chaotic mixer [1]. Freely swimming collections of bacteria have been observed to enhance diffusion and superdiffusive mixing has been measured [10,11].

If a large number of bacteria are encouraged to adhere to a substrate, then a bacterial carpet will be created with unique properties. This was observed by Darnton et al. [7], in which *S. marcescens* were observed to stick to a poly-dimethyl-siloxane (PDMS) film, where they were observed to generate fluid flow motions ("whirlpools" and "rivers") and to enhance the local diffusion of fluorescent tracer particles in the region above the carpet. We suspect that the flow inside a microchannel coated with a bacterial carpet may demonstrate similar properties and the successful demonstration of bacteria as microfluidic actuators in a designed system might be of value in future microfluidic systems. Exploring this possibility forms the central theme of the current paper.

Flagellated bacteria are also exquisitely sensitive to a wide variety of external stimuli. They respond to thermal and chemical gradients that directly influence their motility characteristics and form the basis for chemotactic and thermotactic responses [8]. Changes in temperature or the chemical environment can stimulate the bacteria's sensory system and alter the flagellar motor performance, including the counterclockwise and clockwise rotation intervals and the rotation frequency [12–14]. This sensitivity can be exploited to control the behavior and performance of a bacterial carpet.

One can imagine appliations where it is undesirable to introduce freely swimming bacteria into the working fluid, and thus, in this paper we extend the work of Kim and Breuer [11] to study the use of *bacterial carpets* (rather than freely swimming bacteria) to enhance mixing. Bacterial carpets are surfaces activated by the adhesion of bacteria [7], and thus, the biological cells are not mixed with the working fluid. The current paper is divided into two thrusts in which we (i) explore the possibility of using bacterial carpets to generate enhanced microfluidic mixing and (ii) examine the ability of chemical and thermal signals to control the device's performance by affecting the bacterial behavior. These investigations are conducted using simple microfluidic devices such as flow-through microchannels and sealed microfluidic chambers. This enables careful characterization and comparisons to theory, although the expectation is that these methods can be applied to more complex devices of practical interest.

2 Materials and Methods

2.1 Culturing Bacteria. *S. marcescens* were used in this study: ATCC 274 (American Type Culture Collection, wild type), provided by L. Turner and H. Berg of the Rowland Institute at Harvard University. For the best motility, the 100 μl frozen ali-

[1]Present address: Mechanical Engineering and Mechanics, Drexel University, Philadelphia, PA 19104.
[2]Corresponding author.
Contributed by the Fluids Engineering Division of ASME for publication in the JOURNAL OF FLUIDS ENGINEERING. Manuscript received February 5, 2006; final manuscript received September 7, 2006; Assoc. Editor: Ali Beskok.

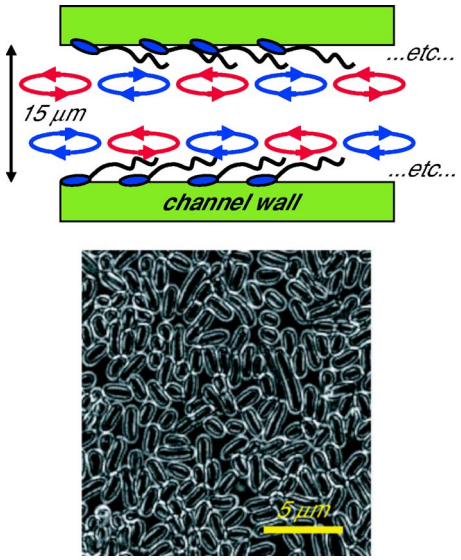

Fig. 1 Schematic of the bacterial mixing system and micrograph of the bacterial carpet as it develops inside the microfluidic system. The picture is taken 2000 s after the initiation of the flow deposition procedure. The scale bar is 5 μm.

quot of *S. marcescens* was put into 10 ml of LB growth medium and incubated for 4 h at 33 °C. The cultures were aerated by gently shaking the tube at ~180 rpm. The bacteria were removed from the incubator during the exponential phase of their growth for use in the experiments. After longer incubation times, the density of the culture saturates and motility quickly decreases. The *S. marcescens* were separated from the nutrient broth by centrifugation at 2200 g for 10 min and then resuspended in 0.5 ml of buffer. Buffer, consisting of 0.01 M KPO_4, 0.067 M NaCl, 10^{-4} M EDTA, (pH 7), was then added to bring the total volume to 10 ml. This separation process was repeated three times to ensure that all the growth medium were removed. The average size of *S. marcescens* is ~1 μm dia by 2 μm long, with 3–5 long (10 μm), thin (20 nm) helical filaments.

2.2 Microfabrication and Formation of Bacterial Carpets. The experiments were conducted using fluid devices fabricated using "soft lithography" techniques [15] in which a geometry is molded using poly-dimethyl-siloxane (PDMS) and then bonded to a glass substrate to form a microfluidic system. The geometries tested were long, wide channels, 15 μm high, 200 μm wide, and several millimeters long. Since these devices are closed, the bacterial carpets were formed on the inside surfaces using flow-deposition techniques rather than the blotting techniques of Darnton et al. [7]. Using a syringe pump, a buffer containing a high concentration ($2-5\times10^9$/ml) of motile *S. marcescens* was pumped through the channel at a low flow rate (0.05 μl/min). After 5 s, the pump was switched off, and the system was allowed to settle for 5 min. During this time, the bacteria swim randomly through the channel, sticking on contact to bare spots on both the PDMS and glass surfaces. *S. marcescens* form slimy durable coatings on the cell body and strongly adhere to the inside of the channel. The flow-and-settle cycle was repeated until the surfaces of the microchannel were coated to the desired density. The system must be rotated to ensure even coating and to counteract the natural tendency for the cells to preferentially coat the lower surface.

The formation of the carpet was tracked optically using differential interference contrast (DIC) microscopy. The DIC image was preprocessed by removing the static background image and then thresholding to enhance the outline of each cell body (Fig. 1). MATLAB-based image processing tools were used to determine the

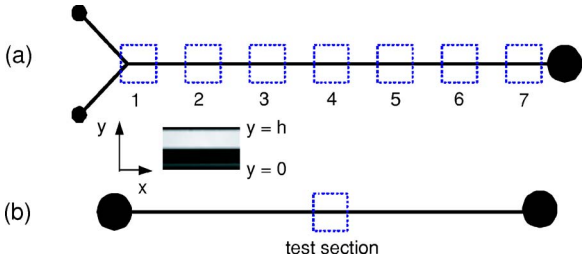

Fig. 2 Schematic of the test geometries: (*a*) the Y-junction microchannel and (*b*) the straight microchannel

cell density ("fill factor") and distributions of the cell orientation. The carpet was largely comprised of a bacterial monolayer, and examination of the carpet images indicated that 81% of the cells adhered to the surface as a single isolated cell, whereas 19% were in contact with or partially on top of another bacterial cell. The most probable orientation of the cells was observed to be parallel to the major axis (x) of the channel, and it was found that 55% of the cells were aligned between −30 deg and +30 deg with respect to the channel's x-axis. After 3000 s, the fill factor was measured to be 83% (±1.2%), and the average density of bacteria was 31/100 μm^2 (±2). Although a few cells were observed to stick to the surface by their flagella, most of the cells stuck to the surface by their bodies with their flagella free to rotate in the flow.

2.3 Experimental methods. The first experiment was designed to observe the mixing of two streams of fluid. This is an extension of the experiments of Kim and Breuer [11] in which freely swimming *E. coli* bacteria were observed to enhance laminar mixing. A PDMS Y-junction microchannel was fabricated, with two arms each feeding a stream of fluid into a main mixing channel that measured 28 mm long, 15 μm high and 200 μm wide (Fig. 2(a)). A *S. marcescens* carpet was flow deposited on the inside of the microchannel and then rinsed with motility buffer. During the experiment, one arm of the Y-channel carried a pure biological buffer solution, with a low concentration (0.02 vol. %) of FITC (Fluorescein isothiocyanate)-labeled Dextran (MW 77,000). The second arm contained the same buffer and Dextran, except that the Dextran was not fluorescently labeled. Images were captured at seven sections located at x=0.5, 4, 8, 12, 16, 20, 24 mm, and at four different flow rates (Q=0.468, 0.376, 0.282, 0.188 μl/min). As the two streams flow down the main channel, a clear boundary between the fluorescent and nonfluorescent streams is established at the Y-junction. The two streams mix together, generating an increasingly diffuse fluorescence profile at x stations further down the channel (Fig. 3). The intensity profile was monitored using a high resolution charged-coupled device (CCD) camera from which the diffusion profiles could be extracted.

Images were obtained using a Nikon TE200 inverted epifluorescent microscope with a 20× objective and recorded with an IDT SharpVision 12-bit cooled CCD camera (IDT, Tallahassee FL), with 1300×1080 pixels. Ten images were recorded at each x station and each flow rate. The intensity profiles across the channel were computed by averaging the ten frames and averaging over 300 pixels in the streamwise direction (corresponding to 107 μm). The maximum of the intensity profile was calculated by fitting the top five data points (two to either side of the peak intensity) to a quadratic polynomial $[y=y_0-a(x-x_0)^2]$. The width of the mixing zone was determined from the standard deviation of the gradient of the intensity distribution, computed by integrating the moments of the intensity gradient distribution using Simpson's rule.

A second experiment was also designed to assess diffusion enhancements in a sealed system. For these experiments, diffusion was measured from the dispersion of tracer particles. A straight

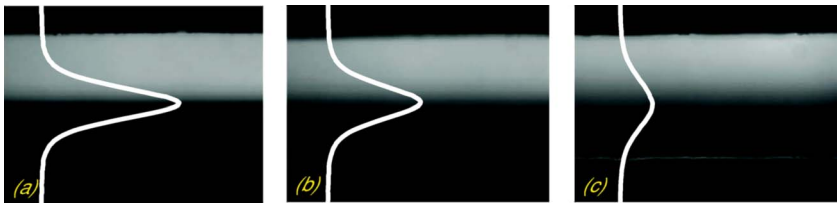

Fig. 3 The photographs illustrate typical intensity distributions in the Y-junction microchannel, showing the diffusion profiles ($\partial I/\partial y$) that is established between the labeled and unlabeled streams (x=24 mm, Q=0.188 μl/min): (*a*) the clean-walled microchannel, (*b*) the channel coated with nonmotile bacterial carpet, and (*c*) the channel coated with an active bacterial carpet. The enhancement of mixing is apparent.

PDMS microchannel (15 mm long) was fabricated with a single inflow and outflow (Fig. 2(*b*)). Following the formation of the bacterial carpet in the straight microchannel, the system was rinsed with the motility buffer to remove drifting bacteria and then seeded with a low concentration (0.04 vol. %) of neutrally buoyant fluorescent particles (490 nm dia Duke Scientific, Palo Alto CA). Finally, the inlet and the outlet were sealed using a drop of RTV silicone adhesive sealant (Permatex, Solon OH).

Mixing is quantified by measuring the effective diffusion coefficient. This is appropriate given the fact that mixing enhancements due to the bacterial carpet are isotropic, continuous, and distributed—all qualities of diffusive processes. Diffusion was determined using particle tracking velocimetry. Image pairs consisting of two successive CCD images (5 ms exposure, separated by 50 ms) were acquired using standard fluorescence microscopy techniques. The fluorescent particles were identified and tracked from the first image to the second, yielding a displacement vector. Approximately 3000 vectors were computed at each condition. Using a 100× objective, the image resolution is 64 nm/pixel, and assuming a tracking accuracy of 0.05 pixels, the displacement resolution is thus 3.2 nm. Typically, 100 image pairs were recorded at a fixed point in the channel in the course of several minutes. Effective diffusion coefficients were then computed from the width of the measured particle displacement distribution.

3 Results and discussion

3.1 Mixing enhancements in a Y-junction channel. Kim and Breuer [11] showed that freely swimming bacteria can enhance the mixing between two streams in a Y-junction microchannel. The present experiment repeats this experiment with the major difference that the bacterial are fixed to the device walls and do not need to be present in the two fluid streams. The evolution of the diffusion interface in the Y-channel can be modeled accurately using a quasi-one-dimensional theory [11] in which the concentration of the fluorescent tracer is represented by the fluorescence intensity, I,

$$\frac{\partial I}{\partial \tau} = D\frac{\partial^2 I}{\partial y^2} \tag{1}$$

where the pseudotime variable, τ, is defined as x/U (U is the average streamwise velocity) and D is the effective diffusion coefficient. This is Fick's second equation, satisfying the initial condition (I=0, $y>0$, and τ=0) and the boundary condition ($I=I_0$, y=0, and $\tau>0$). The solution to this equation is

$$I(\eta) = \mathrm{erfc}(\eta) \tag{2}$$

where η is a similarity variable

$$\eta = \frac{y}{\sqrt{Dx/U}} \tag{3}$$

Thus, the gradient of the intensity profile should behave like

$$\frac{\partial I}{\partial y} = \frac{1}{2\sqrt{\pi Dx/U}} \exp^{-(y/2\sqrt{Dx/U})^2} \tag{4}$$

from which one observes that the maximum in the intensity gradient should decay proportional to $(x/U)^{-1/2}$, and that the width of the diffusion zone, measured by the standard deviation of the intensity gradient, should grow proportional to $(x/U)^{1/2}$. Figure 4 shows the behavior of the maximum of the intensity gradient measured for three cases: (i) a baseline channel with clean walls, (ii) a channel coated with an inactive bacterial carpet, and (iii) a channel coated with an active (motile) bacterial carpet. Images of the intensity profile were obtained for several values of x and U, and the values of the effective diffusion coefficient D were extracted from the composite data using a least-squares regression analysis. Note that the collapse of the data with the similarity variable $\tau = x/U$ is excellent. For this particular carpet (83% fill factor), the effective diffusion coefficient D is observed to increase above the

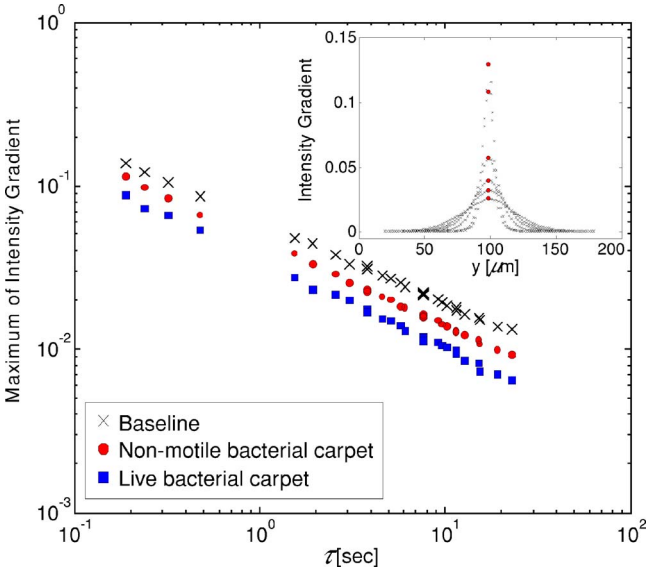

Fig. 4 The variation of the maximum of the intensity gradients, from all seven x locations and four different flow rates. Inset shows the gradient of the intensity profiles at different distance from the Y-junction, generated from images for Q =0.468 μl/min. Fluorescence intensity distributions are extracted from photographs shown in Fig. 3, and plotted against $\tau = x/U$, where U is the average flow velocity. Three sets of data are shown: (i) the clean-walled microchannel, (ii) the channel coated with nonmotile bacterial carpet, and (iii) the channel coated with an active bacterial carpet and the downward shift in each line indicates the increased diffusion due to presence and motion of bacterial flagella. The gradient of the intensity profile decays and spreads as $\tau = x/U$ increases.

baseline value by a factor of four, rising from 21.3 to 85.4 $\mu m^2/s$. After testing with the active bacterial carpet, 0.001% of FCCP (carbonylcyanide-p-trifluoromethoxyphenyl hydrazone) was added to the buffer, rendering the bacteria nonmotile. The channel coated with nonmotile bacterial carpet still resulted in an observed increase in D (to 41.8 $\mu m^2/s$), indicating that the mere presence of the passive flagella in the flow enhances fluid transport. Note that in the 15 μm high channel, the passive flagella (which are approximately 10 μm long) will extend throughout the flow system and their thermal motion will induce some additional transport. Darnton et al. [7] measured rise in the diffusion coefficient of 1 μm beads from 0.48 $\mu m^2/s$ in the bulk to 22.4 $\mu m^2/s$ at the carpet surface. The enhanced values in the present case are even larger, presumably due to the fact that the fluid streams are influenced by flagella from cells on both the top and bottom walls. Similar experiments conducted in a 40 μm deep channel did not show any enhanced transport when the cells were inactive.

The presence of freely swimming bacteria has also been observed to lead to the superdiffusive motion of passive tracer particles [10,11], which mix faster than the square-root dependence predicted by standard Fickian diffusion. Careful analysis of the data in Fig. 4 shows that the maximum in the intensity gradient does decays faster than $\sqrt{\tau}$. We can model the decay in the maximum intensity gradient, I_{max} (normalized by some initial value, I_0) as

$$\frac{I_{max}}{I_0} \propto \left[\frac{\tau^*}{\tau}\right]^{\gamma} \tag{5}$$

where γ is the diffusion exponent and τ^* is a reference time scale. For Fickian diffusion, γ is equal to 0.5, and τ^* is determined solely by the molecular diffusion coefficient D. Applying this model to the current data yields γ=0.499 for the baseline (clean channel) while γ=0.524 and 0.542 for the inactive and active carpets, respectively, indicating a mildly superdiffusive process, and comparable to the values found for freely swimming bacteria in a microchannel [11].

3.2 Mixing Enhancement in a Sealed System. The second series of experiments was designed to explore the dependence of the mixing enhancements on the elapsed time as well as on the composition of the fluid buffer. Since the mixing enhancement is due to the motion of living, motile bacteria, we would expect that the conditions of the buffer solution, its pH, oxygen content, etc., will have an effect on the bacterial carpet's effectiveness. For this experiment, tracer particles were introduced into a straight channel which was then sealed.

Immediately after the carpet creation, beads were observed to move rapidly, and over long distances, consistent with the observations over exposed bacterial carpets [7]. After long times, the bead motion was much more subdued. This motion was characterized by computing an effective diffusion coefficient D_p from the mean-square particle displacement statistics and by comparing D_p to the diffusion coefficient of the same particles due to Brownian motion D_b. This assay was repeated at regular intervals to determine the time-evolution of the carpet's effectiveness. We find that the diffusion enhancement, D_p/D_b, reaches its maximum value D_o immediately after the carpet's formation, after which time it decays exponentially, with a decay rate α (Fig. 5),

$$\frac{D_p}{D_b} = 1 + D_o \exp(-\alpha t) \tag{6}$$

For these conditions, diffusion enhancements in excess of 20 times that due to Brownian motion are achieved and the behavior over time is consistent with the behavior of bacterial carpets in open systems [7].

3.2.1 Effects of Glucose Concentration. These measurements were repeated for a variety of glucose concentrations (0, 2, 20, 60, and 120 mM), two of which are shown in Fig. 5, from which we see that the elevated glucose concentration serves to increase the initial diffusion enhancement D_o, but also to increase the subsequent decay rate α. Figure 6 shows the dependence of the initial diffusion enhancement D_o and the decay rate of the particle diffusion due to bacterial carpets in response to changes in concentration of glucose. A small increase in the buffer glucose concentration quickly increases the initial diffusion coefficient, although as the concentration increases the diffusion coefficient approaches a plateau. This behavior is due to the fact that, although the presence of small concentrations of glucose increases the metabolic rate of the bacteria, resulting in higher motor rotation rates [9,16], the glucose consumption rate per cell quickly saturates at a buffer concentration of ~20 mM, above which the increased concentration has no additional effect on the motor performance. Similar behavior is seen with the decay rate of the diffusion enhancement

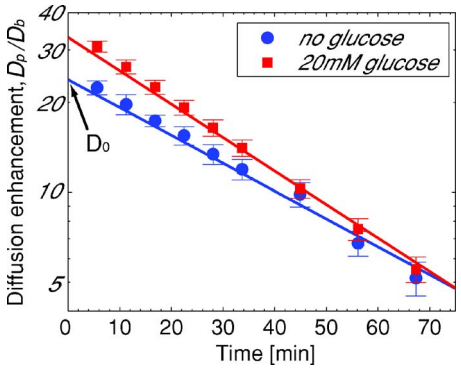

Fig. 5 Enhancement over Brownian motion of the tracer particle diffusion coefficient as a function of time. Two measurement series are shown: with the plain motility buffer (circles) and with 20 mM glucose added (squares). Error bars represent standard deviations based on five sets of measurement.

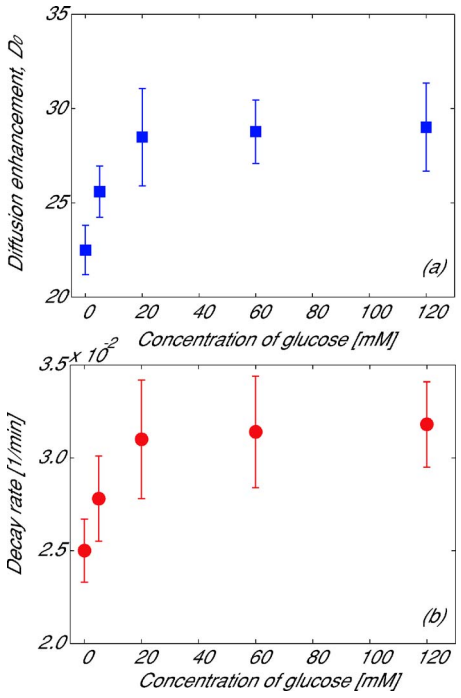

Fig. 6 Variation of (*a*) the initial diffusion enhancement factor and (*b*) the decay rate for flows above bacterial carpets in response to changes in concentration of glucose (0, 2, 20, 60, and 120 mM). Error bars represent standard deviations based on five sets of measurement.

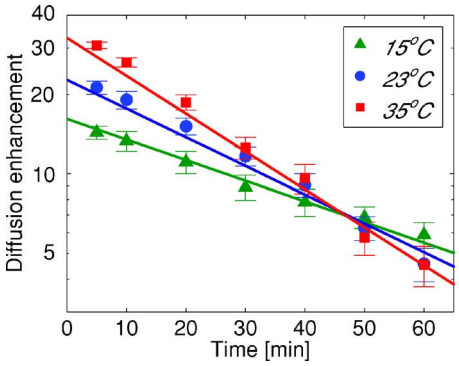

Fig. 7 Enhancement over Brownian diffusion as a function of time at different temperatures. The rising temperatures increase the metabolic activity of the cells resulting in increased diffusion enhancement. However, that increased activity also hastens the carpet's catabolic poisoning, resulting in a faster decay in the mixing activity. Error bars represent standard deviations based on five sets of measurement.

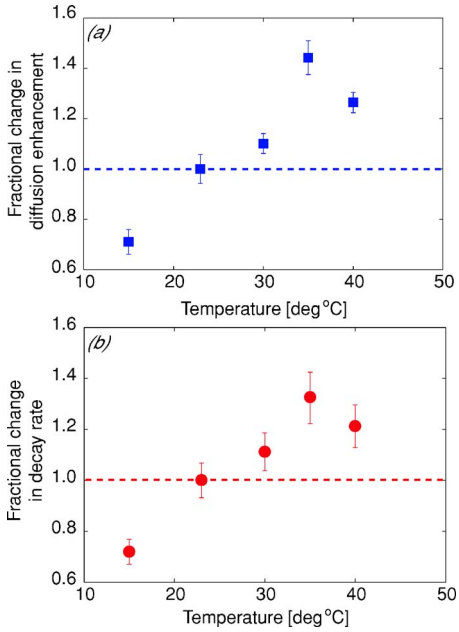

Fig. 8 Percent variation of (*a*) the initial diffusion enhancement and (*b*) the decay rate due to bacterial carpet motility as a function of temperatures. The increase in temperature of the buffer shows an increase in the initial motility and a increase in the decay rate up to 35 °C. The decline at *T*=40 °C may be related to changes in tumbling frequency for *S. marcescens* observed at higher temperatures [16]. Error bars represent standard deviations based on five sets of measurement.

factor. This may be explained by the fact that bacterial catabolism of glucose rapidly produces lactic, acetic, citric, and pyruvic acids in the buffer [17], and since the system is sealed, there is no mechanism to remove these waste products and they cause the buffer pH to drop. Cellular activity, including motor performance is driven by trans-membrane pH gradient and thus, as the pH drops, the cell motility (and thus the carpet motility) falls [8]. Thus in these sealed systems, the carpet's activity directly leads to its own decline and at the elevated metabolic rates induced by the superabundant glucose concentrations, this process is only made more extreme.

Another reason for the decay in the carpet's effectiveness over time may be due to oxygen starvation. For the bacterium, the power required to swim is about 8×10^{-18} W (8×10^{-11} ergs/s), which corresponds to the consumption of oxygen at a rate of ~25 mol/s [18]. However, the introduction of a carbon source, such as glucose, enables cell growth, in which case the rate of oxygen consumption can rise by two orders of magnitude [18]. A reasonable estimate for the amount of dissolved oxygen in the buffer solution at 25°C is 1.6×10^{20} mol/l [19], and taking into account the amount of dissolved oxygen in the sealed microchannel (~7×10^{12} mol) and the number of bacteria that form the carpet (~2×10^{6}, based on a fill factor of bacteria of 31.3/100 μm^2), we can estimate that, in the *absence* of any growth, the oxygen in the sealed system is sufficient to sustain the bacteria for close to 40 h. Thus, in the absence of glucose, the decay of the diffusion enhancement is likely not due to oxygen starvation. However, in the presence of glucose, if the oxygen consumption increases by only a factor of 50, then the bacterial metabolism will become oxygen limited, adding to (indeed dominating) the effects of catabolic poisoning, resulting in the increased decay rate of the diffusion enhancement observed in Fig. 5.

3.2.2 Effects of Temperature. The flagellar motion on the bacterial carpet is also quite sensitive to temperature because an individual bacteria's motility pattern is strongly influenced by the motor rotation frequency and the tumbling frequency, both of which are temperature sensitive [12,16]. Using the procedure described above, the evolution of the effective diffusion enhancements as a function of time were measured at different ambient temperatures (Fig. 7). The percentage deviation from the baseline measurement (at 23°C) of the initial diffusion enhancement D_o and of the decay rate ε is shown in Fig. 8.

In general, the initial diffusion enhancement increases with increasing temperature until it reaches a peak at 35°C. The dip at 40°C might be related to the observed fall in the tumbling frequency at higher temperatures [12], which may lead to reduced hydrodynamic effectiveness, although this needs to be studied further. As with the glucose dependence, the behavior of the diffusion coefficient decay rate follows closely the behavior of the initial diffusion coefficient and strengthens the hypothesis that the reduction in carpet effectiveness is directly caused by the production of metabolic side-products, and that at higher metabolic rates (either due to glucose or temperature effects), increased carpet activity is necessarily accompanied by a faster decline in motility.

4 Conclusions

We have demonstrated the use of a bacterial carpet as a convenient means to enhance mixing in a microfluidic system. The carpet can be easily formed using a flow deposition technique. The random rotation of the flagella acts as a mixer, increasing effective diffusion coefficients by factors in excess of thirty times the baseline diffusion coefficient. The performance of microfluidic devices powered by bacterial carpets has also been shown to be a sensitive function of the environment in which the bacteria live. Factors that enhance bacterial motility, such as the concentration of glucose and the system temperature, affect the carpet motility and hence influence the overall diffusion of the passive tracer. The decline of the device performance is thought to be related to the effects of catabolism in which by-products of the carpet metabolism reduces the buffer pH and hence leads to a reduction in motility and device performance. In addition, oxygen starvation can play a role in a sealed system, particularly when the level of metabolic activity is raised by the addition of a food source such as glucose.

Bacterial carpets are clearly not yet a mature technology. The purpose of this paper is not to suggest that bacterial carpets are ready to displace other more conventional techniques for mixing (such as moving surfaces or electrokinetic systems). Rather we aim to demonstrate that actuators from biological systems such as

bacteria can be effectively harnessed in engineered systems. Effective applications are still some years away and many issues need to be addressed. Comparisons between the *S. Marascens* carpet-based system discussed here, and the mixing achieved by freely-swimming *E. Coli* demonstrated in our earlier work [11] are difficult since the bacteria used have quite different metabolic characteristics. However, the system demonstrated here has many advantages over the free-flowing bacterial mixer, particularly because with the carpet, the cells are not part of the stream, but fixed to the device wall. Such bacterial systems are (to our knowledge) the first demonstrations of biological actuation of an engineered microfluidic system. The robustness, easy of manufacture and the ability to genetically modify their behavior make such systems highly attractive for powering microfluidic devices.

Acknowledgment

This work was supported by the DARPA BioMotors program and the Ostrach Graduate Fellowship (M.J.K.). The assistance and collaboration with Howard Berg, Linda Turner, Nicholas Darnton, Tom Powers, Greg Huber, and MunJu Kim are most gratefully acknowledged.

References

[1] Aref, H., 1984, "Stirring by Chaotic Advection," J. Fluid Mech., **143**, pp. 1–21.
[2] Oddy, M. H., Santiago, J. G., and Mikkelsen, J. C., 2001, "Electrokinetic Instability Micromixing," Anal. Chem., **73**, pp. 5822–5832.
[3] Strembler, M. A., Haselton, F. R., and Aref, H., 2004, "Designing for Chaos, Applications of Chaotic Advection at the Microscale," Philos. Trans. R. Soc. London, Ser. A, **362**, pp. 1019–1036.
[4] Liu, R. H., Stremler, M. A., Sharp, K. V., Olsen, M. G., Santiago, J. G., Adrian, R. J., Aref, H., Bebee, D. J., 2000, "Passive Mixing in a Three Dimensional Serpentine Microchannel," J. Microelectromech. Syst. **9**, 190–197.
[5] Strook, A. D., Dertinger, S. K. W., Ajdari, A., Mezic, I., Stone, A., and Whitesides, G. M., 2002, "Chaotic Mixer for Microchannels," Science, **295**, pp. 647–651.
[6] Tabeling, P., Chabert, M., Dodge, A., Jullien, C., and Okkels, F., 2004, "Chaotic Mixing in Cross-Channel Micromixers," Philos. Trans. R. Soc. London, Ser. A, **362**, 987–1000.
[7] Darnton, N., Turner, L., Breuer, K., and Berg, H., 2004, "Mixing Fluids With Bacterial Carpet," Biophys. J., **86**, pp. 1863–1870
[8] Berg, H. C., 2003, "The Rotary Motor of Bacterial Flagella," Annu. Rev. Biochem., **72**, 19–54.
[9] Manson, M. D., Tedesco, P., Berg, H. C., Harold, F. M., and Van der Drift, C., 1977, "A Protonmotive Force Drives Bacterial Flagella," Proc. Natl. Acad. Sci. U.S.A., **74**, pp. 3060–3064.
[10] Wu, X. L. and Libchaber, A., 2000, "Particle Diffusion in a Quasi-Two-Dimensional Bacterial Bath," Phys. Rev. Lett., **84**, pp. 3017–3020
[11] Kim, M. J. and Breuer, K. S., 2004, "Enhanced Diffusion Due to Motile Bacteria," Phys. Fluids, **16**(9), pp. 78–81.
[12] Maeda, K., Imae, Y., Shioi, J. I., and Oosawa, F., 1976, "Effects of Temperature on Motility and Chemotaxis of Escherichia coli," J. Bacteriol., **127**, pp. 1039–1046
[13] Macnab, R. M., Koshland, R. M., 1972, "The Gradient-Sensing Mechanism in Bacterial Chemotaxis," Proc. Natl. Acad. Sci. U.S.A., **69**, 2509–2512.
[14] Berg, H. C. and Turner, L., 1990, "Chemotaxis of Bacteria in Glass Capillary Arrays," Biophys. J., **58**, pp. 919–930.
[15] Duffy, D., McDonald, C., Schueller, O., and Whitesides, G., 1998, "Rapid Prototyping of Microfluidic Systems in Poly(dimethylsiloxane)," Anal. Chem., **70**, 4974–4984.
[16] Blair, D. F., 1991, "The Bacterial Rotary Motor," Nanotechnology, **2**, pp. 123–133.
[17] Solé, M., Rius, N., and Lorén, J. G., 2000, "Rapid Extracellular Acidification Induced by Glucose Metabolism in Non-Proliferating Cells of Serratia marcescens," Internatl Microbiol, **3**, pp. 39–43.
[18] Berg, H. C., 1993, *Random Walks in Biology* Exp. ed., Princeton University Press, Princeton.
[19] Cui, Y. Q., Van Der Lans, R. G. J. M., and Luyben, K. C. A. M., 2000, "Effects of Dissolved Oxygen Tension and Mechanical Forces on Fungal Morphology in Submerged Fermentation," J. Bacteriol., **57**, pp. 409–419.